Trajectory Shifts in the Arctic and Subarctic Freshwater Cycle

Bruce J. Peterson,[1*] James McClelland,[2] Ruth Curry,[3] Robert M. Holmes,[4] John E. Walsh,[5] Knut Aagaard[6]

Manifold changes in the freshwater cycle of high-latitude lands and oceans have been reported in the past few years. A synthesis of these changes in freshwater sources and in ocean freshwater storage illustrates the complementary and synoptic temporal pattern and magnitude of these changes over the past 50 years. Increasing river discharge anomalies and excess net precipitation on the ocean contributed ~20,000 cubic kilometers of fresh water to the Arctic and high-latitude North Atlantic oceans from lows in the 1960s to highs in the 1990s. Sea ice attrition provided another ~15,000 cubic kilometers, and glacial melt added ~2000 cubic kilometers. The sum of anomalous inputs from these freshwater sources matched the amount and rate at which fresh water accumulated in the North Atlantic during much of the period from 1965 through 1995. The changes in freshwater inputs and ocean storage occurred in conjunction with the amplifying North Atlantic Oscillation and rising air temperatures. Fresh water may now be accumulating in the Arctic Ocean and will likely be exported southward if and when the North Atlantic Oscillation enters into a new high phase.

The hydrologic system, including precipitation minus evaporation (P-E), terrestrial ice, sea ice, and ocean circulation, is a major component of ongoing changes in land and ocean ecosystems of the Arctic (*1*). Precipitation at high latitudes is increasing (*2*, *3*), river discharge is rising (*4*), glaciers (*5*) and the Greenland Ice Sheet (*6*) are shrinking, and the sea ice cover of the Arctic Ocean is decreasing in both thickness and extent (*7*). In recent decades, the Nordic Seas and Subpolar Basins experienced a remarkable freshening (*8*–*10*). Half of the total freshening occurred rapidly during the early 1970s, a period called the Great Salinity Anomaly (GSA) (*11*), but the freshening continued at a lesser rate until the late 1990s (*10*). These manifold changes in the freshwater (FW) system were largely synchronous and correlated with the amplifying North Atlantic Oscillation (NAO) index and rising air temperatures that characterized the period 1950–2000 (*2*–*4*, *12*). Here, we synthesize these observations in order to mechanistically link the Arctic FW system to the North Atlantic, including its subtropical basins.

To focus our synthesis, we pose a simple question: Can the increases in FW inputs from both atmospheric moisture convergence and from melting Arctic ice account for the recently documented freshening of the North Atlantic? Our approach is to calculate annual and cumulative FW input anomalies from net precipitation (P-E) on the ocean surface, river discharge (P-E on land), net attrition of glaciers, and Arctic Ocean sea ice melt and export for the latter half of the 20th century and compare these fluxes to measured rates of FW accumulation in the Atlantic's Nordic-Subpolar-Subtropical basins (hereafter NSSB) during the same period. These are estimates and budgets of FW anomalies (changes in fluxes and stocks relative to defined baselines during the years 1936–1955) and not budgets of total FW fluxes and stocks (*13*). A recent review of the Arctic Ocean FW budget (*14*) complements this review of changes in the FW cycle.

The domain for this synthesis (Fig. 1) includes the Arctic Ocean and its watershed, the Canadian Archipelago, Baffin Bay, Hudson Bay and its watershed, the Nordic Seas, Subpolar Basins, and the deep (>1500 m) subtropical basins of the North Atlantic. Anomalies of FW inputs were estimated by using the sources in Table 1 and compared to estimates of FW storage that were previously reported for the Nordic and Subpolar Seas (*10*) but here expanded to incorporate the deep Subtropical Basins (*13*). The present analysis of river discharge supplements previous reports of sustained Eurasian river runoff increases since the late 1960s (*4*, *15*) by incorporating the entire Arctic Ocean watershed and updating the records through 2003. Bering Strait plays a substantial role in the Arctic FW budget but is excluded here because long-term (1955–2000) changes in FW transport are unknown (*16*, *17*). A lack of adequate salinity data precludes assessing changes in the total FW content of the Arctic Ocean, although some information is available on changes in upper ocean

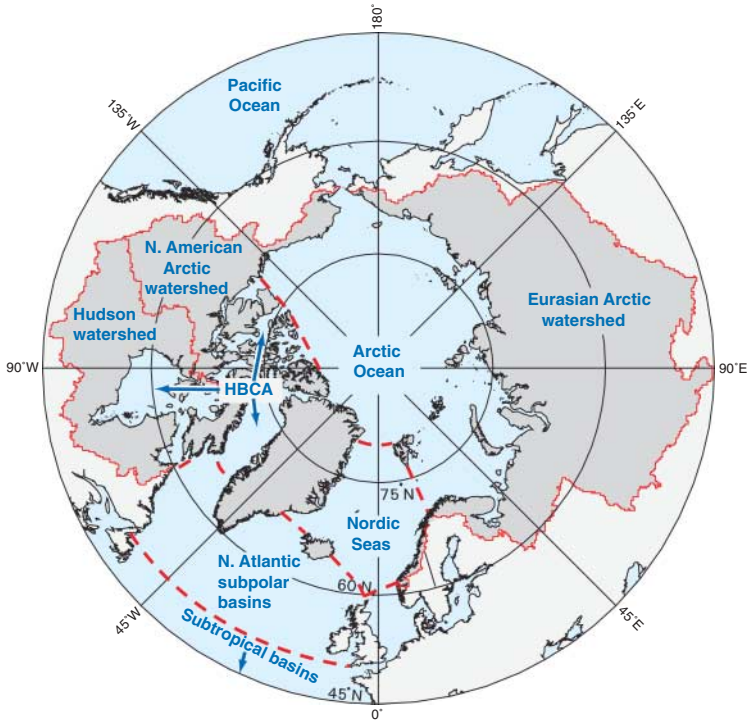

Fig. 1. Polar projection map showing the watershed and ocean domains used for estimates of freshwater anomalies. Solid red lines delineate watershed boundaries used for calculations of river discharge anomalies. Dashed lines separate regions of the ocean surface used for calculations of P-E anomalies and define the boundaries used for freshwater storage analysis in the Nordic Seas and the North Atlantic Subpolar Basins (*10*).

[1]Ecosystems Center, Marine Biological Laboratory, Woods Hole, MA 02543, USA. [2]Marine Science Institute, University of Texas at Austin, Port Aransas, TX 78373, USA. [3]Woods Hole Oceanographic Institution, MS 21, Woods Hole, MA 02543, USA. [4]Woods Hole Research Center, 149 Woods Hole Road, Falmouth, MA 02540, USA. [5]International Arctic Research Center, 930 Koyukuk Drive, Post Office Box 75340, Fairbanks, AK 99775, USA. [6]Applied Physics Laboratory, University of Washington, 1013 NE 40th Street, Seattle, WA 98105, USA.

*To whom correspondence should be addressed. E-mail: peterson@mbl.edu

Table 1. Contemporary anomalies for major FW sources to the Arctic Ocean, HBCA, Nordic Seas, and Atlantic Subpolar Basins. Anomalies for river discharge and P-E are relative to a 1936–1955 baseline. Anomalies for small glaciers and ice caps include melt from the pan-Arctic watershed, Arctic and subarctic islands, and ice caps around but not connected to the Greenland Ice Sheet. Anomalies for sea ice focus specifically on melting of stocks in the Arctic Ocean. Anomalies for small glaciers and ice caps, the Greenland Ice Sheet, and sea ice are relative to a water balance of zero (no net change in volume). In all cases, positive values indicate excess FW inputs to the ocean. Dashed entries indicate no estimates. R-ArcticNET v3.0 is a river discharge archive, and ERA-40 is a reanalysis of atmospheric observations.

Freshwater sources	References	Years covered in references	Avg. anomaly ± SE for 1990s (km^3 $year^{-1}$)	% relative to 1936–1955 baseline
Rivers flowing into the Arctic Ocean	Peterson *et al.* (*4*) R-ArcticNET v3.0 (*55*) Wu *et al.* (*14*)	1936–1999 2000–2003 1900–2050	163 ± 34	+5.3
Rivers flowing into Hudson Bay	Déry *et al.* (*56*)	1964–2000	−59 ± 16	−8.0
Small glaciers, ice caps	Dyurgerov and Carter (*5*)	1961–2001	38 ± 13	—
Greenland Ice Sheet	Box *et al.* (*6*)	1991–2000	81 ± 38	—
P-E, Arctic Ocean	ERA-40 (*57*)	1958–2001	124 ± 72	+7.6
P-E, HBCA	ERA-40 (*57*)	1958–2001	81 ± 33	+15.6
P-E, Nordic Seas	ERA-40 (*57*)	1958–2001	67 ± 28	+17.8
P-E, Subpolar Basin	ERA-40 (*57*)	1958–2001	336 ± 73	+16.8
Sea ice	Rothrock *et al.* (*7*)*	1987–1997	817 ± 339	—
TOTAL			1649	

*Rothrock *et al.* (*7*) reported observed changes in sea ice thickness annually from 1987–1997 and also modeled changes over a wider time frame (1951–1999). Thickness has been converted to freshwater volume following Wadhams and Munk (*58*).

salinities (*18*). Complete mass balance estimates for the Greenland Ice Sheet are not available for the entire 1955–2000 period; thus, only its recent (1990s) and potential future FW contributions are discussed (*2*, *3*, *6*, *19*, *20*).

Freshwater Anomalies

Estimates of flux and cumulative volumetric anomalies are given for eight different FW sources (Fig. 2 and Table 1) (*13*): river discharge to the Arctic Ocean and to Hudson Bay, P-E over the Arctic Ocean and over the Hudson Bay–Baffin Bay–Canadian Archipelago open water region (hereafter HBCA), Arctic glacier melt (excluding the Greenland Ice Sheet), Arctic sea ice attrition (*21*), and P-E over the Nordic Seas and Subpolar Basins. Of the individual records, sea ice exhibited the greatest interannual variability in flux anomalies (±1200 km^3 $year^{-1}$ for 5-year averages) and the largest amplitude of cumulative change over the record (15,000 km^3, expressed as net FW melt equivalent). Summed over the entire spatial domain, however, the change in combined cumulative P-E anomalies (ocean P-E plus runoff from land) from their lowest values in 1965–1970 to peak values in the year 2000 was ~20,000 km^3, somewhat larger than sea ice input. Arctic glacier melt (excluding Greenland) played a relatively small but growing role in the total anomaly history (*5*). Greenland's massive ice sheet has also exhibited net shrinkage in recent years (*6*, *19*). Its average net melt during the 1990s was estimated at ~80 km^3 $year^{-1}$ (*6*) (Table 1) but appears to have recently increased to ~220 km^3 $year^{-1}$ (*20*).

Despite increasing FW contributions to the Arctic Ocean during the latter half of the 20th century, the near-surface layers of the Arctic Ocean became saltier (*18*). This increase in salinity suggests that the anomalous FW contributions were exported along with an additional quantity of FW drawn from Arctic Ocean storage [Supporting Online Material (SOM) text]. Swift *et al.* (*18*) described salinity increases in the upper 175 m of the Arctic Ocean between the periods 1949–1975 and 1976–1993. These salinity increases were evident in all areas of the Arctic Ocean except parts of the Makarov and the northeasternmost Canada basins [boxes 9 and 13, figure 1 in (*18*)]. By using the data of Swift *et al.* (*18*), we calculate that depth-weighted mean salinity increased in the 0- to 50-m layer by 0.39 practical salinity units (psu), in the 50- to 100-m layer by 0.11, and in the 100- to 175-m layer by 0.05, with little change at greater depths. The salinity increase between the midpoints of the 1945–1975 and the 1976–1993 periods was equivalent to a withdrawal of ~4000 km^3 of FW at a rate of ~180 km^3 $year^{-1}$. However, the sparsity of available data precludes further assessment of Arctic Ocean volumetric changes with any confidence.

FW storage in the NSSB over the years 1953–2003 experienced a net gain of ~17,000 km^3, which included an initial loss of ~8000 km^3 in the 1950s and early 1960s followed by a sustained period of FW accumulation of ~25,000 km^3 from 1965 to 1995 (Fig. 3C). The greatest rate of accumulation, ~10,000 km^3 in a 5-year period, occurred in the 1970s, the time of the GSA.

Of the three NSSB regions, the largest and most rapid changes occurred in the Subpolar Basins (Fig. 3C). Although the bulk of Arctic sea ice and other FW exports flow southward through Fram Strait, only a small part spreads from the East Greenland Current into the interior of the Nordic Seas, with most being transported directly through Denmark Strait into the Subpolar Basins (*22*). Almost no excess FW entered the deep Subtropical Basins until after 1987 (Fig. 3C), when deep convection in the Subpolar Basins produced extremely cold but fresh, dense waters. All of the FW anomalies exported to the subtropics (total ~9000 km^3) were stored at depths > 1500 m. Of this total, about half accumulated below 2200 m and is linked to upstream changes in the products of Nordic Seas overflows and entrainment that ventilate these deep subtropical basins. The other half, which accumulated at depths between 1500 to 2200 m, is linked to changes in Labrador Sea water properties (*23*).

Collectively comparing the FW source and ocean FW sink records, two features of the histories emerge: (i) the overall synchrony of changes and (ii) their timing relative to changes in global surface air temperature (SAT), the NAO index, and the associated Northern Annular Mode (NAM) index (*24*) (Figs. 2 and 3). Although year-to-year comparisons of FW sources and sinks are largely impractical (*25*), the synchrony of trajectories and shifts across the individual records suggests dividing the timeline (T) into four periods: T1, the years before the GSA period (through 1965), characterized by a persistent negative NAO phase and relatively cool global SAT; T2, the GSA period itself (1966–1980), with multiyear oscillations of the NAO and a transition to increasing SAT; T3, the subsequent years (1981–1995), when the NAO was in a positive phase and the global SAT was rising; and T4, the years after the 1995–96 retreat of the NAO to a neutral phase, during which SAT continued to increase.

Concomitant changes in all of the major FW input anomalies near the T1-T2 boundary (Fig. 2) indicate an abrupt trajectory shift in the Arctic and Subarctic FW cycle during the late 1960s to early 1970s. This trajectory shift was associated with sharply increased P-E over the Subpolar Basins, Nordic Seas, Arctic Ocean, and HBCA region (Fig. 2). Simultaneously, Eurasian river discharge began to exhibit positive anomalies, while Hudson Bay river discharge began to diminish. Sea ice, which had been accumulating in the Arctic Ocean from 1950 to 1965, reversed direction in 1965 to a variable but sustained decline over subsequent decades (*7*).

Over the next 30 years, T2 and T3, the NAO index and global air temperatures trended upward with decadal bumps, the individual FW sources fluctuated in harmony, and cumulative FW inputs largely paralleled ocean storage. This synchrony in FW sources and NSSB storage, however, did not hold completely after 1995, period T4, when the NAO and the NAM retreated to more neutral values while global and arctic SAT continued to rise (*26*). Near-surface waters in the Subpolar Basins and Nordic Seas became more saline (*27*) as P-E over the ocean domains declined, but anomalies of river discharge to the Arctic Ocean (primarily Eurasian discharge) remained strongly positive and river discharge anomalies to Hudson Bay became positive. Glacial and Greenland Ice Sheet melting continued at an accelerated pace (*5*, *19*), and sea ice reached record area minima in summer and winter (*28*). Increasing river discharge and melting rates of sea ice and glaciers during recent years appear to be coupled with increasing temperature, whereas the ocean P-E anomalies remain closely tied to the dynamics governing the NAO and the NAM.

Atmospheric Moisture Flux Convergence

The cumulative contributions of (i) local P-E (Subpolar and Nordic Seas), (ii) remote P-E (Arctic Ocean–HBCA P-E plus Arctic Ocean–Hudson Bay river discharge), (iii) sea ice, and (iv) glacier melt were summed and compared to the cumulative NSSB FW storage anomalies by normalizing all records to 1965, when the entire system shifted and ocean FW storage was lowest (Fig. 4 and Table 2). The sum of all P-E anomalies (local plus remote) (Fig. 4) constituted half (~16,000 km^3) of the total FW collectively added since 1965, and with the exception of the years 1986–1988 the annual flux anomalies were uniformly positive in sign between 1970–2000, in contrast to negative anomalies that prevailed before 1970. This trajectory shift in atmospheric moisture flux convergence onto the high northern latitudes complemented FW losses from the low-latitude Atlantic, Pacific, and Indian oceans that were diagnosed through salinity changes over the same time period (*9*, *29*, *30*) and the large-scale mid-latitude drying since 1998 documented for the Northern Hemisphere (*31*). The preponderance of evidence indicates that a global redistribution of FW has taken place. Whether or not this involved increased global rates of total evaporation, precipitation, and atmospheric moisture transport, i.e., an acceleration of the entire global hydrologic cycle, remains undetermined.

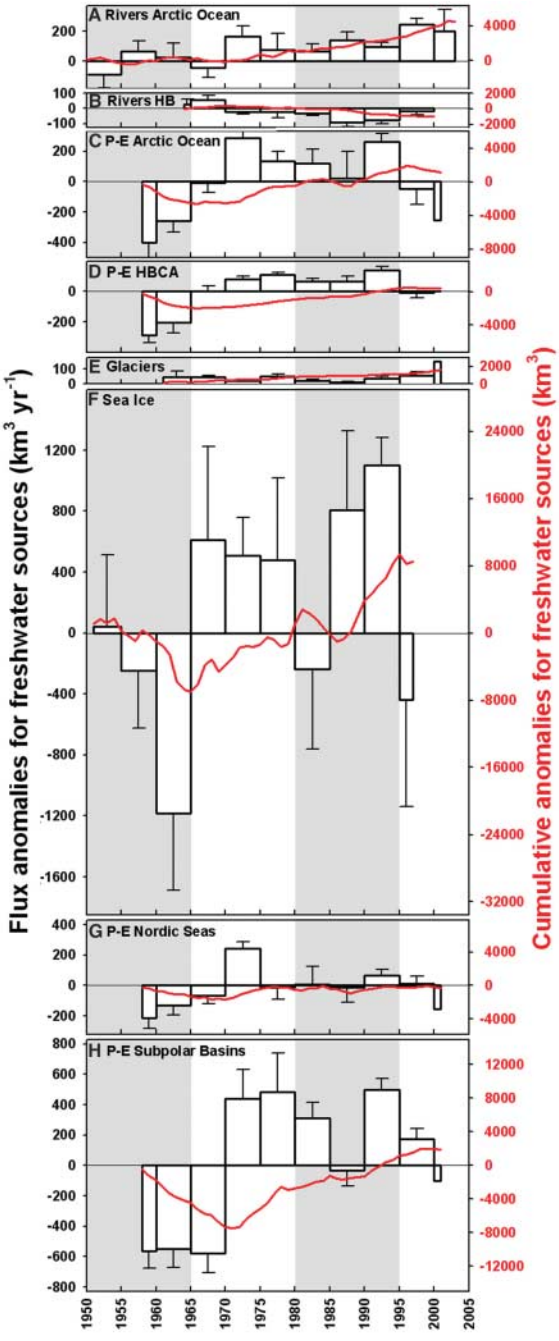

Fig. 2. Time course of FW source anomalies. (**A**) River discharge into Arctic Ocean, (**B**) river discharge to Hudson Bay, (**C**) P-E over Arctic Ocean, (**D**) P-E over HBCA, (**E**) glacier melt (excluding Greenland), (**F**) Arctic Ocean sea ice attrition, (**G**) P-E over Nordic Seas, and (**H**) P-E over Subpolar Basins. Bars show average anomalies and standard errors for 5-year increments, except when data are not available for the full period. In these cases, the narrower width of the bars reflects the number of years in the average. The continuous red lines represent cumulative freshwater anomalies (scale on right-hand axis). Positive anomalies represent excess FW inputs to the ocean. The alternating white and gray areas delineate time intervals that are discussed in the text (T1 to T4) when comparing source anomaly patterns to changes in ocean storage.

Annual P-E fluxes within the individual Arctic and subarctic domains and within the overall domain (remote plus local) exhibit decadal variability that tracks the NAO index. This relationship was previously noted for Eurasian and Hudson Bay river discharges (*4*, *32*), P-E onto the Nordic and Subpolar Seas (*33*), and atmospheric moisture flux convergence into the polar cap north of 70°N (*34*). Although specific details of the dynamics governing the NAO and the NAM remain elusive, their amplification in recent decades may reflect a nonlinear response to rising greenhouse gas concentrations and ozone depletion through a variety of mechanisms. These include stratospheric cooling and intensification of the polar vortex (*35*, *36*), Arctic sea ice loss (*37*), and atmospheric teleconnections to elevated Indian Ocean sea surface temperatures (*38*, *39*) and are part of a growing body of evidence suggesting that factors are aligning to favor continued amplification of the NAO and the NAM, and thus elevated amounts of P-E at the high latitudes, in the 21st century (*26*).

Arctic Ocean FW Exports

The Arctic FW budget includes an average oceanic FW influx from the Pacific of ~2500 km^3 year^{-1} (*17*) and FW and sea ice exports to the North Atlantic of ~8000 km^3 year^{-1} (*40*–*42*), with the balance (~5500 km^3 year^{-1}) supplied by atmospheric moisture flux convergence over the Arctic Ocean and its watershed (*14*). Direct measurement of these fluxes is difficult, and their interannual variability remains uncertain. However, the consequences of variability in Arctic Ocean export are visible as interannual changes in Arctic sea ice volume and as North Atlantic FW pulses such as the GSA. Several studies have suggested that these changes are choreographed by a broad-scale dynamical system that alternately accumulates FW and sea ice in the Arctic and exports them to the North Atlantic (*43*–*46*). The mechanism involves changes in strength of the Arctic high sea level pressure (SLP) cell leading to Arctic Ocean circulation regimes, which alternately favor retention and release of sea ice and FW. To the extent that Arctic SLP is governed by the same processes that control the NAO and the NAM, one should expect Arctic FW exports and the NAO and the NAM to be linked.

The sparse Arctic Ocean observational record precludes direct verification of this dynamical framework, but the timing and the magnitude of Arctic FW release episodes can be diagnosed by comparing the NSSB storage history to local and remote FW sources. The NSSB FW budget is maintained by three essential components: (i) local P-E on the Nordic and Subpolar Seas, (ii) horizontal FW fluxes from the Arctic and the HBCA, and (iii) saline ocean inflows from the subtropics. After removing the local P-E contribution, the residual FW storage anomaly represents the net sum of oceanic fresh and saline inflows. A positive FW residual implies a dominance of Arctic inflow, a negative FW residual implies a dominance of subtropical inflow, and a zero residual implies a net balance between them.

The cumulative FW storage and local P-E diverge after 1965, with local P-E inputs accounting for less than 30% of the changes in NSSB FW storage from 1965 to 2000 (Fig. 4). Net changes in FW sources, storage, and residuals (NSSB storage minus local P-E) were computed for each period (Table 2). The residuals indicate periods of enhanced (T2 and T3) and diminished (T4) Arctic FW influences on the NSSB storage anomaly history. Cumulative FW input and storage were about equal during T2 and T3, whereas cumulative input exceeded storage during T1 and T4, implying that excess FW was accumulating in the Arctic during those periods [although no estimates of FW melt equivalent are available for the continued sea ice attrition reported after 1997 (*28*)].

During T1, the NAO and the NAM were in a negative phase and trending downward, NSSB FW storage declined at a rate of ~400 km^3 year^{-1}, and sea ice and FW were both accumulating in the Arctic. Over the next 30 years (T2 and T3), the NAO and the NAM were trending upward to a persistently high phase, and NSSB FW storage increased dramatically (average rate of +800 km^3 year^{-1} but episodic), accounting for nearly the entire sum of anomalous FW source inputs. The NAO and the NAM switched to extreme low values in 1995–1996 but did not settle into a persistent high or low phase thereafter (T4), and the sum of available FW source inputs increased slightly. This excess of Arctic FW had little net influence on the NSSB FW storage, which declined at a rate of ~400 km^3 year^{-1}, implying that Arctic FW exports also retreated with the NAO index. Marked changes did occur in the Subpolar Basins as saline subtropical surface waters flowed into the subpolar and Nordic circulations (*27*), but about half of the subpolar FW losses were matched by FW gains in the subtropical deep basins. The relatively small net FW decrease (residual ~ –2700 km^3) over the entire NSSB system during T4 implies that subtropical saline inflows slightly exceeded Arctic FW inflows from 1995 onward. The larger implication is that the FW presently accumulating in the Arctic will find its way into NSSB storage if and when the atmospheric circulation patterns re-establish a weakened Arctic high SLP and positive NAO and NAM phase.

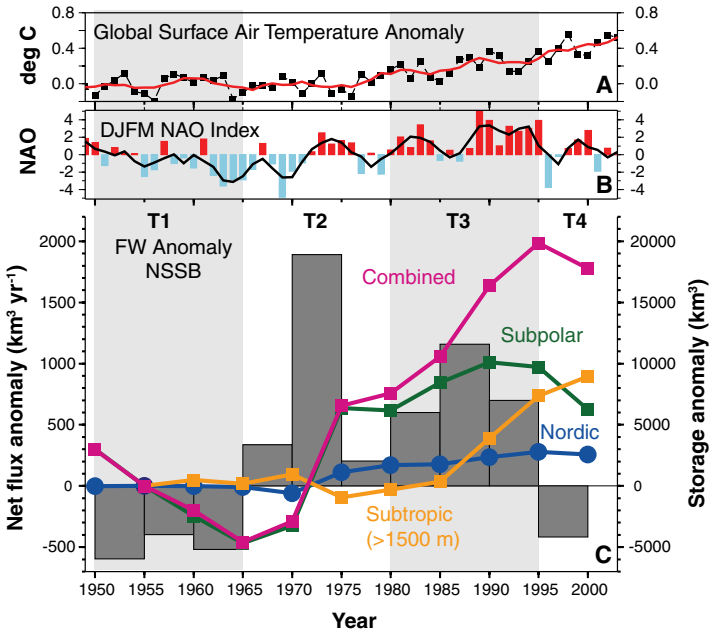

Fig. 3. North Atlantic Ocean FW storage anomalies, NAO index, and global surface temperature anomaly, 1950–2005. Gray shading delineates four time periods (T1 to T4) described in text. (**A**) Global SAT anomalies (*53*). Black dashed curve and symbols are annual anomalies; red curve is 5-year running mean. (**B**) Winter [December through March (DJFM)] NAO index (*54*). Blue and red bars are annual index values; black curve is 5-year running mean. (**C**) FW storage anomalies (km^3) relative to 1955 for Nordic Seas (blue), Subpolar Basins (green), deep (>1500 m) Subtropical Basins (orange), and all regions combined (purple). Ocean anomalies represent 5-year averages and center on years marked with symbols. Bars denote net flux anomalies (km^3 year^{-1}), computed as difference in storage between consecutive time periods.

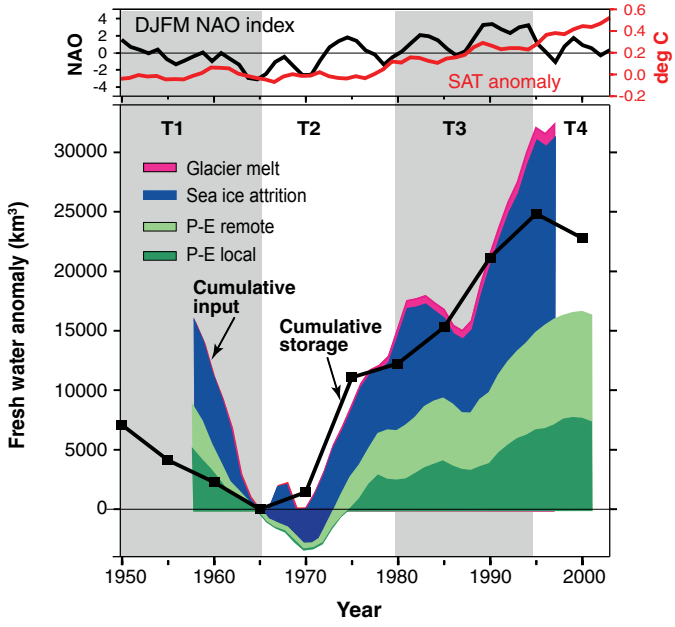

Fig. 4. Comparison of FW source anomalies and FW storage anomalies relative to 1965 (units are km^3). Black curve is cumulative NSSB ocean FW storage. Colored areas represent cumulative FW contributions from P-E local (Subpolar plus Nordic Seas, dark green), P-E remote (Arctic Ocean, HBCA, and river discharge, light green), sea ice attrition (blue), and glacier melt (red). Source contributions are stacked to show total FW source input.

Meridional Overturning Circulation

Numerous modeling studies have identified mechanisms linking North Atlantic salinity distributions to changes in strength of the meridional overturning circulation (MOC). An abundant literature exists on this topic, and the interested reader is referred to (*47*–*49*) as a starting place. If changes in the MOC's northward transport of subtropical saline surface waters were governing the NSSB FW storage variability, we might infer a weakening of the MOC between 1965–1995, when residual FW storage (after removing the local P-E contributions) and therefore the net oceanic FW influx increased. However, the subtropical surface waters themselves were characterized by increased salinities in this time period (*9*), ruling them out as a likely source of the FW anomaly. Indeed, simulations of 20th century climate using HadCM3 reproduced the high-latitude freshening, traced its source to Arctic sea ice and in-

Table 2. Approximate volumetric FW gains or losses (in km³) for each time period and various FW source or sink components. T1, T2, and T3 span 15 years each, T1a is the subset of T1 for which P-E estimates are available, and T4 encompasses the post-1995 period for which measurements are available. P-Eremote is the sum of Arctic Ocean P-E, HBCA P-E, Arctic rivers, and Hudson rivers. P-Elocal is the sum of Nordic Seas and Subpolar Basins P-E. Storage – P-Elocal is referred to in text as residual NSSB FW gain or loss. Question marks identify time periods where data coverage was not sufficient for calculations.

	1951–1965 T1	1958–1965 T1a	1966–1980 T2	1981–1995 T3	1996–2001 T4
Sea ice attrition	–7000	–6000	+8000	+8400	?
Glacier melt	?	?	+600	+300	+400
Arctic Ocean P-E	?	–2500	+2100	+2000	–500
HBCA P-E	?	–1900	+1000	+1400	0
Arctic rivers	0	+500	+1000	+1500	+1500
Hudson rivers	?	?	+100	–1000	–100
P-Eremote	?	–3800	+4100	+3900	+800
P-Elocal	?	–5700	+2500	+4200	+700
NSSB storage	–7100	–4100	+12,200	+12,600	–2000
Storage – P-Elocal	?	+1600	+9700	+8400	–2700

creased river runoff, and diagnosed a slightly enhanced MOC over this same time period (*49*).

In more than 2 decades of direct measurements, the MOC's principal source currents, the northward flow of warm surface waters through Florida Strait (*50*) and the southward flows of cold, dense waters from the Nordic Seas across Denmark Strait and through the Faroe Bank Channel, have not exhibited sustained changes in flow strength. The eastern overflow did appear to slow for a few years between 1999 and 2001 but recovered its usual strength in subsequent years (*10*). Although Bryden *et al.* (*51*) reported evidence for a recent (post-1998) MOC weakening across 25°N, the transport changes estimated in that study are very near the error limits of the calculation. Moreover, the reported MOC slackening was accompanied by salinity increases in the near-surface layers of the eastern Subpolar and Nordic Seas (Fig. 3 and fig. S1) (*27*), opposite in sign to expectations. Rather, the overall balance between anomalous FW inputs and ocean FW storage suggests that Arctic exports, governed by atmospheric circulation modes and warming, dominated the observed NSSB freshening from 1965–1995 without need to invoke changes in the MOC. Those exports declined after 1995, and subtropical saline influences began to dominate the net storage changes in the NSSB at about the same rate (–400 km³ year^{-1}) as was the case between 1950–1965.

Thus, although we cannot exclude a role for changes in the MOC in the observed freshening of the North Atlantic, the overall agreement between anomalous FW inputs and changes in ocean FW storage suggests that increased high-latitude FW inputs were primarily responsible for the observed freshening during 1965–2000.

Present and Future Implications

Variability observed in the high-latitude hydrologic system reflects interplay of SAT and atmospheric circulation patterns. The Arctic, HBCA, Nordic, and Subpolar regions are all affected by global SAT, because SAT influences high-latitude moisture flux convergence, and by regional SAT, because SAT influences cryosphere melt. Atmospheric modes, such as the NAO and the NAM, modulate the pathways that redistribute atmospheric moisture, affect regional temperature regimes, and orchestrate the circulation of sea ice and surface waters in the Arctic Ocean. These modes play an important role in the timing and magnitude of North Atlantic freshening through their impacts on local P-E and on the alternate accumulation and release of sea ice and FW from the Arctic Ocean and HBCA into the NSSB.

In the 2000s, pervasive changes have continued to modify the Arctic hydrologic system in ways that reflect both the neutral state of the NAO and the NAM and the influence of rising temperatures. Sea ice continued to decline (*28*) despite the post-1995 retreat of the NAO and the NAM and probable reduced Arctic exports to the NSSB, the surface waters of the Beaufort Gyre exhibited widespread freshening (*52*), and melting of the Greenland Ice Sheet accelerated (*19*). Although meltwater contributions from Arctic glaciers and the Greenland Ice Sheet have thus far played a relatively minor role in the FW anomaly record, rising temperatures will undoubtedly amplify that contribution in potentially dramatic ways (*20*). As we look to future decades, the interplay between the NAO and the NAM and the continuation of global greenhouse warming will determine whether the Arctic–North Atlantic FW cycle continues its upward trend of increasing high-latitude FW inputs and ocean FW storage or shifts once again to a new trajectory.

References and Notes

1. J. T. Overpeck *et al.*, *Eos* **86**, 309 (2005).
2. J. T. Houghton *et al.*, Eds., *Climate Change 2001: The Scientific Basis. Contribution of Working Group I to the Third Assessment Report of the IPCC* (Cambridge Univ. Press, Cambridge, 2001).
3. ACIA 2005, *Arctic Climate Impact Assessment: Scientific Report* (Cambridge Univ. Press, Cambridge, in press).
4. B. J. Peterson *et al.*, *Science* **298**, 2171 (2002).
5. M. B. Dyurgerov, C. L. Carter, *Arct. Antarct. Alp. Res.* **36**, 117 (2004).
6. J. E. Box, D. H. Bromwich, L. S. Bai, *J. Geophys. Res.* **109**, 10.1029/2003JD004451 (2004).
7. D. A. Rothrock, J. Zhang, Y. Yu, *J. Geophys. Res.* **108**, 10.1029/2001JC001208 (2003).
8. R. R. Dickson *et al.*, *Nature* **416**, 832 (2002).
9. R. Curry, B. Dickson, I. Yashayaev, *Nature* **416**, 826 (2003).
10. R. Curry, C. Mauritzen, *Science* **308**, 1772 (2005).
11. R. R. Dickson, J. Meincke, S.-A. Malmberg, A. J. Lee, *Prog. Oceanogr.* **20**, 103 (1988).
12. M. C. Serreze *et al.*, *Clim. Change* **46**, 159 (2000).
13. Materials and methods are available as supporting material on *Science* Online.
14. M. C. Serreze *et al.*, *J. Geophys. Res.*, in press.
15. P. Wu, R. Wood, P. Stott, *Geophys. Res. Lett.* **32**, 10.1029/2004GL021570 (2005).
16. R. A. Woodgate, K. Aagaard, T. J. Weingartner, *Geophys. Res. Lett.* **32**, 10.1029/2004GL021880 (2005).
17. R. A. Woodgate, K. Aagaard, *Geophys. Res. Lett.* **32**, L02602 (2005).
18. J. H. Swift, K. Aagaard, L. Timokhov, E. G. Nikiforov, *J. Geophys. Res.* **110**, 10.1029/2004JC002312 (2005).
19. R. B. Alley, P. U. Clark, P. Huybrechts, I. Joughin, *Science* **310**, 456 (2005).
20. E. Rignot, P. Kanagaratnam, *Science* **311**, 986 (2006).
21. Sea ice attrition is defined as melt plus export, whereas negative attrition equals accumulation plus import.
22. K. Aagaard, E. C. Carmack, *J. Geophys. Res.* **94**, 14485 (1989).
23. R. G. Curry, M. S. McCartney, T. M. Joyce, *Nature* **391**, 575 (1998).
24. D. W. J. Thompson, J. M. Wallace, *Science* **293**, 85 (2001).
25. Comparisons between FW inputs and ocean accumulation for short intervals (5 years) in Fig. 4 must be made with care. The FW source anomaly calculations are based on annual fluxes, and cumulative points represent net contributions through the year at which they are plotted. Points for FW storage in the NSSB are estimated from 5-year average ocean salinity fields and are centered on the middle year of each pentad (for example, the average of storage estimates for 1958–1962 is plotted at 1960). Thus, the timing of input and storage events in Fig. 4 are an indication of events happening in roughly, but not exactly, the same time frame. The FW source and storage estimates do not permit tracking FW dynamically as it moves through the system. Comparing cumulative volumes in general circumvents this deficiency and issues of time lags between FW input and downstream ocean storage.
26. M. Serreze, J. A. Francis, *Clim. Change* **76**, 241 (2006).
27. H. Hátún, A. B. Sandø, H. Drange, B. Hansen, H. Valdimarsson, *Science* **309**, 1841 (2005).
28. W. Meier, J. Stroeve, F. Fetterer, K. Knowles, *Eos* **86**, 326 (2005).
29. A. P. S. Wong, N. L. Bindoff, J. A. Church, *Nature* **400**, 440 (1999).
30. H. L. Bryden, E. L. McDonagh, B. A. King, *Science* **300**, 2086 (2003).
31. M. Hoerling, A. Kumar, *Science* **299**, 691 (2003).
32. S. J. Déry, E. F. Wood, *Geophys. Res. Lett.* **32**, 10.1029/2005GL022845 (2005).
33. S. A. Josey, R. Marsh, *J. Geophys. Res.* **110**, 10.1029/2004JC002521 (2005).
34. A. N. Rogers, D. H. Bromwich, E. N. Sinclair, *J. Clim.* **14**, 2414 (2001).
35. D. Shindell, D. Rind, N. Balachandran, J. Lean, P. Lonergan, *Science* **284**, 305 (1999).
36. D. W. J. Thompson, J. M. Wallace, G. Hegerl, *J. Clim.* **13**, 1018 (2000).
37. V. Semenov, L. Bengtsson, *Geophys. Res. Lett.* **30**, 1781 (2003).
38. J. W. Hurrell, M. P. Hoerling, A. S. Phillips, T. Xu, *Clim. Dyn.* **23**, 371 (2004).
39. M. P. Hoerling, J. W. Hurrell, T. Xu, *Science* **292**, 90 (2001).

40. M. P. Meredith *et al.*, *Geophys. Res. Lett.* **28**, 1615 (2001).
41. S. J. Prinsenberg, J. Hamilton, *Atmos. Ocean* **43**, 430101 (2001).
42. T. Vinje, N. Nordlund, A. Kværnbekk, *J. Geophys. Res.* **103**, 10437 (1998).
43. A. Y. Proshutinsky, M. A. Johnson, *J. Geophys. Res.* **102**, 12493 (1997).
44. A. Y. Proshutinsky, R. H. Bourke, R. A. McLaughlin, *Geophys. Res. Lett.* **29**, 2100 (2002).
45. I. G. Rigor, J. M. Wallace, R. L. Colony, *J. Clim.* **15**, 2648 (2002).
46. L. Mysak, S. Venegas, *Geophys. Res. Lett.* **25**, 3607 (1998).
47. J. Marotzke, *Proc. Natl. Acad. Sci. U.S.A.* **97**, 1347 (2000).
48. S. Rahmstorf, *Clim. Dyn.* **12**, 799 (1996).
49. P. Wu, R. Wood, P. Stott, *Geophys. Res. Lett.* **31**, L02301 (2004).
50. M. O. Baringer, J. C. Larsen, *Geophys. Res. Lett.* **28**, 3179 (2001).
51. H. L. Bryden *et al.*, *Nature* **438**, 655 (2005).
52. A. Proshutinsky *et al.*, *Eos* **86**, 368 (2005).
53. Global SAT values were taken from the National Climatic Data Center (www.ncdc.noaa.gov/oa/climate/research/anomalies/anomalies.html).
54. NAO index values were taken from the National Center for Atmospheric Research (www.cgd.ucar.edu/cas/jhurrell/indices.info.html).
55. Combined discharge from the six largest Eurasian rivers reached a record high of 2060 km^3 $year^{-1}$ in 2002. Data was compiled from R-ArcticNET (www.r-arcticnet.sr.unh.edu/v3.0).
56. S. J. Déry, M. Stieglitz, E. C. McKenna, E. F. Wood, *J. Clim.* **18**, 2540 (2005).
57. S. M. Uppala *et al.*, *Q. J. R. Meteorol. Soc.* **131**, 2961 (2005).
58. P. Wadhams, W. Munk, *Geophys. Res. Lett.* **31**, L11311 10.1029/2004GL020039 (2004).
59. This paper is dedicated to J. E. Hobbie, who introduced the senior author to the study of Arctic fresh waters. We thank B. Chapman for calculations of P-E. Funding was provided by NSF (grants OPP-0229302, OPP-0436118, OPP-0327664, OPP-0352754, OPP-0519840, and OCE-0326778), Office of Naval Research (grant N00014-02-1-0305), and NASA (grant IDS-03-0000-0145).

Supporting Online Material

www.sciencemag.org/cgi/content/full/313/5790/1061/DC1
Materials and Methods
SOM Text
Fig. S1
Table S1

10.1126/science.1122593